

## Disruption of the Mucus Barrier by Topically Applied Exogenous Particles

Shayna L. McGill\* and Hugh D. C. Smyth

*Division of Pharmaceutics, University of Texas at Austin, College of Pharmacy,  
1 University Station A1920, Austin, Texas 78712, United States*

Received July 23, 2010; Revised Manuscript Received September 20, 2010; Accepted  
October 4, 2010

**Abstract:** The mucus barrier is well established as a formidable barrier to exogenous substances and forms the first line of defense for mucosal surfaces. Drugs and particle systems are known to be significantly hindered via a variety of interactions with mucus, and some efforts have been reported that can mitigate these interactions. We investigated topically applied particulate systems (nano and micro) for their potential to interact with mucus and influence on the diffusion of model drugs across the mucus barrier. Functionalized polystyrene nanoparticles and microparticles and diesel particulate matter were topically applied to established in vitro mucus models. Particle treated mucus was then assessed, compared to controls, for drug permeation rates. The average permeation rate of drugs increased 2-fold following the application of particles to mucus compared to permeation of the same drug through mucus alone. In some cases permeation enhancement of small model drugs was over 5 times that of controls. Assessment of particle physicochemical properties also indicated that significant interactions occurred between mucus and the particles as determined by zeta potential changes and size changes. Collectively this work supports the hypothesis that topically applied particles interact with the mucus barrier causing disruption of this barrier allowing for increased drug permeation. These findings have implications for improved drug delivery and enhanced environmental exposure to exogenous substances.

**Keywords:** Mucus; particles; drug delivery; diffusion

### Introduction

Physical barriers such as skin and mucus membranes are the first line of defense for the innate immune system.<sup>1</sup> Mucosal epithelial surfaces such as the nasopharynx, lungs, reproductive tissues, and gastrointestinal organs are protected by a layer of mucus that can trap exogenous substances until they can be removed by clearance mechanisms such as ciliary movement.<sup>1</sup> To successfully perform this role of protection mucus maintains a complex molecular composition and structure.<sup>2</sup> The main component that is responsible for its

viscous and elastic gel-like properties is the glycoprotein mucin.<sup>2</sup> These mucins are large molecules (0.5–20 MDa) that are highly glycosylated. These oligosaccharide chains (5–15 monomers) are attached to a protein core to form a so-called “bottle brush” configuration.<sup>2,3</sup> The chemical composition results in electrostatic, hydrophobic, and hydrogen bonding interactions. It is therefore not surprising that many different interactions can occur between exogenous substances and the adhesive mucus which significantly influence diffusion of solutes through this complex network structure.<sup>2,3</sup>

\* To whom correspondence should be addressed. Mailing address:  
Division of Pharmaceutics, University of Texas at Austin,  
College of Pharmacy, 1 University Station A1920, Austin, TX  
78712-0126. E-mail: smcgill@mail.utexas.edu. Tel: 512-471-  
4752. Fax: 512-471-7474.

(1) Smith, B. T. In *Concepts in Immunology and Immunotherapeutics*,  
4th ed.; Smith, B. T., Ed.; American Society of Health-System  
Pharmacists: Bethesda, MD, 2007.

(2) Bansil, R.; Turner, B. Mucin structure, aggregation, physiological  
functions and biomedical applications. *Curr. Opin. Colloid  
Interface Sci.* **2006**, *11* (2–3), 164–170.

(3) Huang, Y.; Peppas, N. A. Nanoscale Analysis of Mucus-Carrier  
Interactions for Improved Drug Absorption. In *Nanotechnology  
in Therapeutics: Current Technology and Applications*; Peppas,  
N. A., Hilt, J. Z., Thomas, J. B., Eds.; Horizon Bioscience:  
Norfolk, U.K., 2007; pp 109–127.

The importance of the mucus barrier in health and disease is well documented.<sup>2,4–7</sup> Several studies have shown that the transport of certain drugs may be significantly inhibited through mucus.<sup>8–10</sup> In the gastrointestinal tract, it is well established that the mucus layer is the first line of defense against secreted acid and pepsin.<sup>6</sup> This stable unstirred layer forms a diffusion barrier to pepsin, preventing proteolysis of the underlying epithelial cells. In peptic ulcer disease the rate of peptic degradation of the mucus barrier is increased. Moreover, other damaging agents such as ethanol and aspirin can rapidly permeate the mucus barrier, and may induce ulcers by damaging the underlying epithelium. Similarly, in the respiratory epithelium, the presence of mucus has been shown to significantly limit the effectiveness of viral gene therapy vectors.<sup>11–13</sup> In another example of the functional properties of the mucus barrier several groups have studied the entrapment and transport of nanoparticles in cervical mucus and cystic fibrosis mucus samples.<sup>14–17</sup>

Despite this recognition of the formidable barrier and importance of the mucus lining on epithelial surfaces for drug

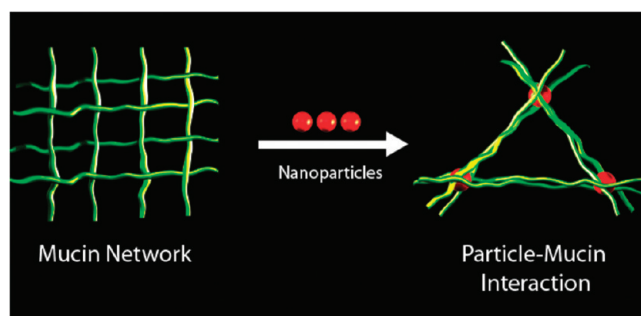


**Figure 1.** A scheme of particle induced disruption of mucus. A mucus fiber network is depicted at left with the introduction of particles (center) leading to an entanglement of particles with mucus resulting in a change of the fiber network.

delivery and solute diffusion, relatively few studies have investigated what external factors may influence its integrity.<sup>18,19</sup>

In the studies reported in this paper, for the first time to our knowledge, we demonstrate that topically applied particles can significantly disrupt the mucus barrier. We demonstrate this disruption phenomenon in established models of mucus using nanoparticles, microparticles, and diesel particulate matter, and the phenomenon is diagrammed in Figure 1. The effects of these particles on mucus were assessed using two model drug species. In addition, we provide evidence of how the particles may interact with mucus to induce such changes in the rate of diffusion of low molecular weight drugs.

## Materials and Methods

**Materials.** Sigma mucin from porcine stomach type 2 and type 3 were used for the models of mucus (type 2 M2378-100G, batch 019K1222, Sigma Aldrich, St. Louis, MO; type 3 M1778-10G, batch 098K7025, Sigma Aldrich, St. Louis, MO). Four particle types were purchased from Invitrogen: FluoSpheres carboxylate- and amine-modified microspheres 1  $\mu\text{m}$  yellow-green fluorescent (F8823, Lot 543029, Invitrogen, Eugene, OR; F8765, Lot 434725, Invitrogen, Eugene, OR); FluoSpheres carboxylate- and amine-modified microsphere 0.2  $\mu\text{m}$  (200 nm) red fluorescent (F8810, Lot 459418, Invitrogen, Eugene, OR; F8763, Lot 531683, Invitrogen, Eugene, OR). Diesel particulate matter was supplied by Jacob McDonald (Lovelace Respiratory Research Institute, Albuquerque, NM). Fluorescein sodium salt (fluorescein; F6377, batch 064K0153, Sigma Aldrich, St. Louis, MO) and

- (4) Thornton, D. J.; Sheehan, J. K. From Mucins to Mucus: Toward a More Coherent Understanding of this Essential Barrier. *Proc. Am. Thorac. Soc.* **2004**, *1*, 54–61.
- (5) Girod, S.; Zahm, J. M.; Plotkowski, C.; Beck, G.; Puchelle, E. Role of the Physicochemical Properties of Mucus in the Protection of the Respiratory Epithelium. *Eur. Respir. J.* **1992**, *5*, 477–487.
- (6) Allen, A.; Hutton, D. A.; Leonard, A. J.; Pearson, J. P.; Sellers, L. A. The Role of Mucus in the Protection of the Gastrointestinal Mucosa. *Scand. J. Gastroenterol.* **1986**, *21*, 71–78.
- (7) Slomiany, B. L.; Slomiany, A. Role of Mucus in Gastric Mucosal Protection. *J. Physiol. Pharmacol.* **1991**, *42*, 147–161.
- (8) Bhat, P.; Flanagan, D.; Donovan, M. Drug binding to gastric mucus glycoproteins. *Int. J. Pharm.* **1996**, *134* (1–2), 15–25.
- (9) Khanvilkar, K.; Donovan, M.; Flanagan, D. Drug transfer through mucus. *Adv. Drug Delivery Rev.* **2001**, *48* (2–3), 173–193.
- (10) Saltzman, W.; Radomsky, M.; Whaley, K.; Cone, R. Antibody diffusion in human cervical mucus. *Biophys. J.* **1994**, *66* (2), 508–515.
- (11) Stonebraker, J. R.; Wagner, D.; Lefensty, R. W.; Burns, K.; Gendler, S. J.; Bergelson, J. M.; Boucher, R. C.; O’Neal, W. K.; Pickles, R. J. Glycocalyx restricts adenoviral vector access to apical receptors expressed on respiratory epithelium in vitro and in vivo: role for tethered mucins as barriers to luminal infection. *J. Virol.* **2004**, *78*, 13755–13768.
- (12) Ferrari, S.; Geddes, D.; Alton, E. Barriers to and New Approaches for Gene Therapy and Gene Delivery in Cystic Fibrosis. *Adv. Drug Delivery Rev.* **2002**, *54*, 1373–1393.
- (13) Laube, B. The expanding role of aerosols in systemic drug delivery, gene therapy, and vaccination. *Resp. Care* **2005**, *50* (9), 1161.
- (14) Sanders, N.; DE SMEDT, S.; Van Rompaey, E.; Simoons, P.; De Baets, F.; Demeester, J. Cystic Fibrosis sputum. A barrier to the transport of nanospheres. *Am. J. Respir. Crit. Care Med.* **2000**, *162*, 1905–1911.
- (15) Dawson, M.; Wirtz, Hanes, J. Enhanced viscoelasticity of human cystic fibrosis sputum correlates with increasing microheterogeneity in particle transport. *J. Biol. Chem.* **2003**, *278*, 50393–50401.
- (16) Lai, S.; O’Hanlon, D.; Harrold, S.; Man, S.; Wang, Y.; Cone, R.; Hanes, J. Rapid transport of large polymeric nanoparticles in fresh undiluted human mucus. *Proc. Natl. Acad. Sci. U.S.A.* **2007**, *104* (5), 1482.

- (17) Olmsted, S.; Padgett, J.; Yudin, A.; Whaley, K.; Moench, T.; Cone, R. Diffusion of macromolecules and virus-like particles in human cervical mucus. *Biophys. J.* **2001**, *81* (4), 1930–1937.
- (18) Lai, S.; Wang, Y.; Cone, R.; Wirtz, D.; Hanes, J. Altering mucus rheology to “solidify” human mucus at the nanoscale. *PLoS One* **2009**, *4* (1), 1–6.
- (19) Bhaskar, K.; Gong, D.; Bansil, R.; Pajevic, S.; Hamilton, J.; Turner, B.; LaMont, J. Profound increase in viscosity and aggregation of pig gastric mucin at low pH. *Am. J. Physiol.* **1991**, *261* (5), 827.

rhodamine B (R6626, batch 063K3406, Sigma Aldrich, St. Louis, MO) were used as model drugs.

**Mucus Models.** The mucus models used in these studies have been widely employed in other permeability studies.<sup>8,20</sup> A 20% w/v concentration of type 3 (unpurified) was mixed with double distilled water in a shaking incubator overnight. A cystic fibrosis sputum model was modified from that of Dawson et al. Briefly, using the type 2 (partially purified) mucin at 60 mg/mL was mixed with 3.2 mg/mL lecithin, which was used in replace of the phosphatidylcholine, and 32 mg/mL BSA in buffer containing 05 mM Na<sup>+</sup>, 75 mM Cl<sup>-</sup>, 20 mM Hepes, pH 7.4, for 48 h.<sup>20</sup>

**Rheological Characterization of Mucus Models.** Dynamic oscillatory measurements were performed at controlled deformation using a TA Instruments AR-G2 Rheometer (TA Instruments, New Castle, DE). Storage, loss, and complex moduli were measured as a function of both deformation and frequency. The linear viscoelastic region was determined with strain sweep under strain amplitude from 0.08 to 10% at a frequency of 10 Hz; frequency sweeps were performed over two frequency intervals (0.1–50 Hz and 0.5–15 Hz) at constant strain (0.5). The linear region was the region of strain by which no yielding of the substances occurs, and the determination of the characteristic relaxation time can occur from the strain sweep test.

**Physical Characterization of Particles.** Prior to characterization of particles using dynamic light scattering and zeta potential, particles were placed either within mucus or in buffer (PBS, pH 7.4). For both conditions particles were exposed to centrifugation at 1200 rpm for 30 min. Then they were washed at least three times with buffer. After each washing step the particles were centrifuged again, to ensure that any non-adhering or non-interacting mucus was removed.

Nanoparticle hydrodynamic diameters were characterized using a ZetaPlus Zeta Potential Analyzer with a Multi Angle Particle Sizing Option installed (Brookhaven Instruments Corporation, Holtsville, NY) operating with a 25 mW laser at a wavelength of 635 nm. Detection of scattered light was at 90° to the incident beam. Each sample was subjected to three 2 min measurements. Typically, solutions of up to  $2 \times 10^{-4}$  mg/mL in 1 mM KCl were used for the characterizations, at a temperature of 25 °C.

ζ-Potential measurements were conducted using electro-phoretic light scattering, also using the Brookhaven ZetaPlus, on the same samples that were sized. Scattered light was detected at 15° (175° to the incident beam) at a temperature of 25 °C. Each sample was subjected to 10 measurements, with a 5 s delay between each measurement.

A Supra 40VP (Carl Zeiss SMT AG, Germany) scanning electron microscope (SEM) was used to determine the morphology of the synthesized particles. Samples were prepared for imaging by drop drying onto an aluminum stage. To prevent charging of the samples, they were sputter coated

with platinum/palladium using a Cressington 208 benchtop sputter coater (Watford, U.K.).

Specific surface area of diesel particulate matter was obtained using the BET method on a Quantachrome Monosorb (Quantachrome Instruments, Florida). Diesel particulates were degassed at 80 °C for 12 h under nitrogen gas flow of 20 psi. Following degassing particulates were analyzed. Specific surface area of monodisperse spheres was determined using calculation of their surface area based on their well-defined size and known densities.

**Permeability Experiments.** Permeability of fluorescein or rhodamine B was determined by using a modified diffusion cell setup. The diffusion cell setup consisted of Snapwells inserts that have surface areas of 1.12 cm<sup>2</sup>, that act as the donor side, placed atop 24 well tissue culture plates containing 3 mL of PBS buffer as the acceptor side (Corning Snapwells, CLS3802, Corning, NY; Multiwell Primaria 24 well, Falcon, Becton Dickinson Labware, Franklin Lakes, NJ). Mucus models were plated onto the Snapwells inserts at a volume of 250 μL, which was sufficient to cover the inserts. Particles were applied topically followed by the topical application of the model drugs fluorescein or rhodamine B. Samples were removed from the acceptor side at predetermined time points and analyzed using a plate reader set up for fluorescence intensity measurements at excitation and emission of 460 and 515 nm for fluorescein and 514 and 630 nm for rhodamine B (Infinite M200, Tecan Group LTD, Männedorf, Switzerland).

Permeability rates (cm/s) were calculated using an Excel spreadsheet (Microsoft Office 2008, version 12.25, Microsoft Corp.). For statistical evaluation of the data, analysis of variance (one-way) and post hoc comparisons (Tukey method) were performed using StatPlus (StatPlus:Mac2009, AnalystSoft).

## Results

Representative examples of the rheological properties of the two *in vitro* mucin models, unpurified reconstituted and CF sputum buffered mucin, are given in Figures 2a and 2b. Elastic ( $G'$ ) and viscous ( $G''$ ) moduli of the two mucus models are presented as functions of oscillatory frequencies.

Particles were characterized using SEM (Figures 3a, 3b). The uniform monodisperse size (200 nm and 1 μm) and shape (spherical) as claimed by manufacturer's specification were confirmed for polystyrene beads. Due to the uniformity of the beads, the specific surface area was calculated using the known density of polystyrene. The surface area for the 200 nm particles was 28.6 m<sup>2</sup>/g and 5.7 m<sup>2</sup>/g for the 1 μm particles. Diesel particulate matter (DPM) was also characterized using SEM (Figure 3c) and dynamic light scattering (mean diameter 287 nm). The specific surface area for the DPM was determined to be 45.0 ± 0.5 m<sup>2</sup>/g as determined by BET measurements.

Drug permeability studies were performed using the unpurified mucin model using either fluorescein or rhodamine B as model drugs under various experimental conditions.

(20) Dawson, M.; Krauland, E.; Wirtz, D.; Hanes, J. Transport of polymeric nanoparticle gene carriers in gastric mucus. *Biotechnol. Prog.* **2004**, *20* (3), 851–857.

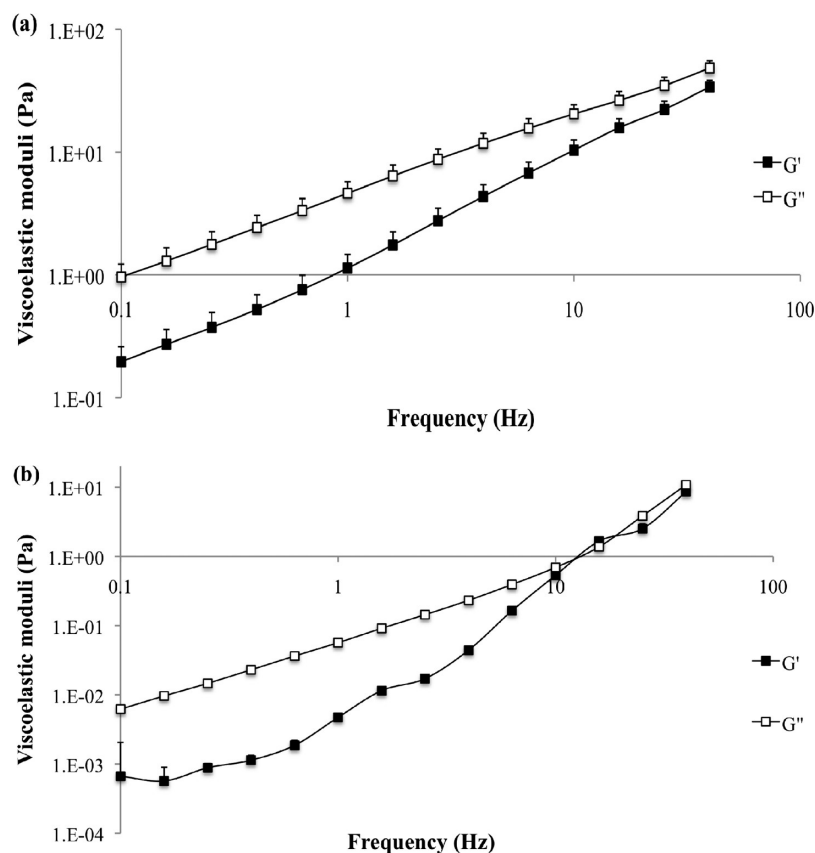


**Figure 2.** Frequency sweep of the mucus model (a) and cystic fibrosis model (b).  $G'$  and  $G''$  are plotted against frequency.

When the polystyrene particles (carboxyl functionalization) were topically added to the mucus model, fluorescein permeability rates were increased 2.4-fold for 200 nm particles and 1.6-fold for 1  $\mu\text{m}$  particles compared to untreated controls (Figure 4a). Rhodamine B exhibited permeability increases of 4.9-fold and 1.6-fold when particles of 200 nm and 1  $\mu\text{m}$ , respectively, were added (Figure 4b), though overall rhodamine B permeability was generally less than that of fluorescein.

The influence of different surface functionalization of the particles on drug permeability was also assessed. Particles functionalized with either amine or carboxyl groups were used and topically applied to the mucus model prior to drug permeation studies. The surface charges of these particles range between 0.1 and 2 mequiv/g, and therefore they remain stable in relatively high concentrations of electrolytes.<sup>21</sup> Permeation rate of fluorescein increased through the mucus model when treated with either amine or carboxyl particles (Figure 5a). For the study performed using rhodamine B as the model drug, overall permeation increases of the drug compared to controls were observed but no significant differences in rates from the different particle types were observed (Figure 5b).

To assess the mucus barrier disruption more generally, an additional mucus model was selected for comparison. This

model, named cystic fibrosis like mucus (or CF mucus), is also derived from literature reports in which researchers have sought to mimic mucus in CF by preparing the in vitro mucus that has similar composition to that of CF patients' sputum samples.<sup>20</sup> In Figures 6a and 6b, a comparison of the permeability enhancement ratios for mucus models, drugs, particle sizes, and particle types is presented. Mucus barrier disruption as measured by the permeation enhancement ratio of the hydrophilic model drug, fluorescein, was no different when comparing the two mucus models. However, significant differences in rhodamine B permeation enhancement ratio were detected due to the differences in the mucus model composition.

The permeation enhancement of each drug as a result of mucus barrier disruption by the different particle sizes is shown in Figure 7. For 1  $\mu\text{m}$  particle treatments, either amine or carboxyl functionalized, no differences were observed between fluorescein or rhodamine B permeation enhancement. Smaller 200 nm particles appear to have a more significant effect (statistical differences detected for both rhodamine and fluorescein), but the magnitude of enhancement was greater for rhodamine B.

To probe particle–mucin interactions on the molecular scale, DLS particle size measurements and zeta potential were performed on particles before and after association with mucus (Figure 8). Particles were treated either with mucin or control (buffer), and then the particles were washed extensively by repeated centrifugation. Strongly bound mucin

(21) Working with FluoSpheres® Fluorescent Microspheres: Properties and Modifications. *Molecular Probes: Invitrogen detection technologies*. Product Information, 2004; pp 1–5.



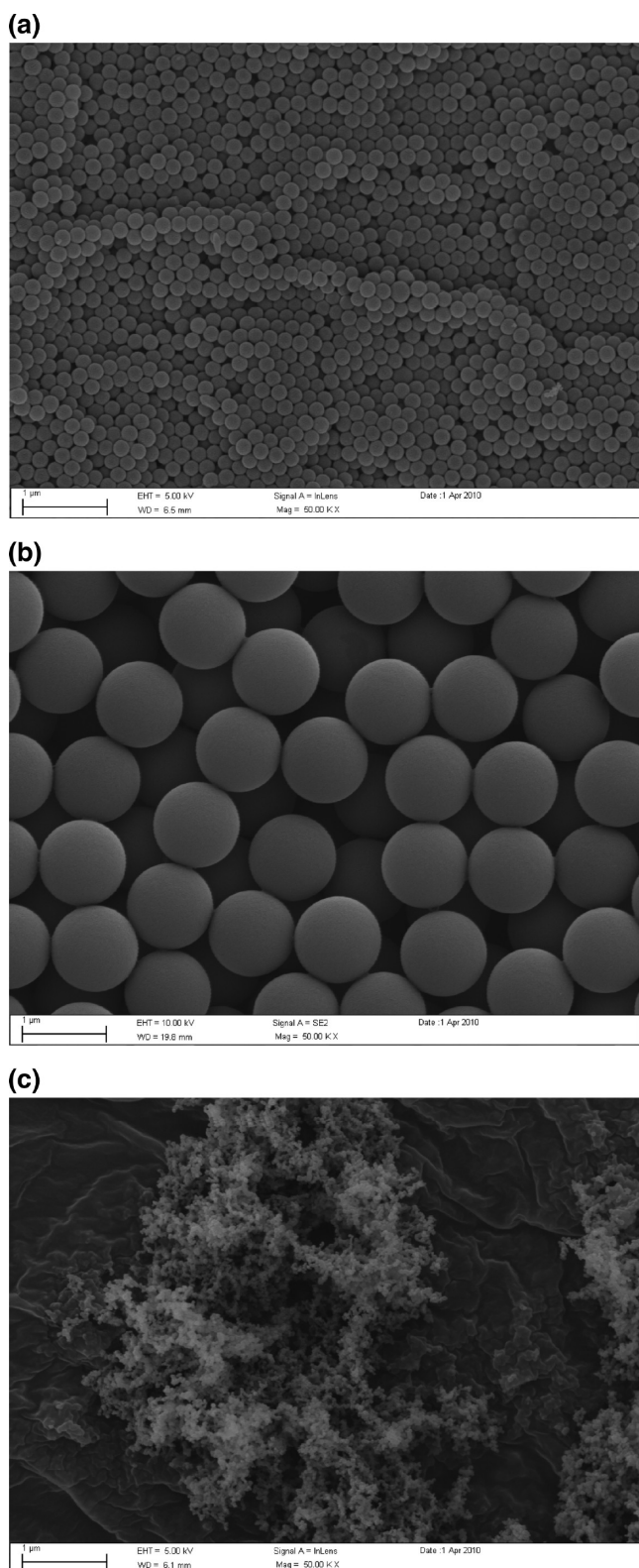


**Figure 3.** SEM images of carboxyl-modified 200 nm (a) and 1  $\mu\text{m}$  (b) particles, and diesel particulate matter (c) were obtained at 50000 $\times$  magnifications.

molecules on the particle surfaces could therefore be detected using both size and charge measurements performed on the washed particles. Both amine and carboxyl particles treated in mucin had significant increases in particle size compared

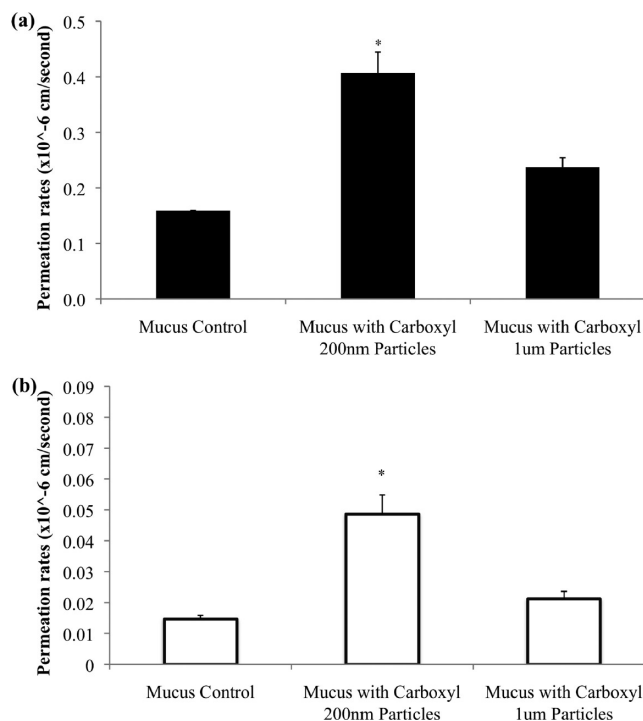


**Figure 4.** The effect of carboxylated particle size (200 nm versus 1  $\mu\text{m}$ ) on permeation rates across a mucus model determined for fluorescein (a) and rhodamine B (b). For both drugs statistically significant ( $p < 0.05$ ) differences were found for the 200 nm particles when compared to permeation rates of controls and 1  $\mu\text{m}$  particles.

to particles that were only treated in buffer (Figure 8a). The zeta potentials were also found to significantly change (to similar magnitudes) for both particle types after mucin treatment (Figure 8b).

To extend our investigations further, mucus models were then topically treated with diesel particulate matter (instead of monodisperse polystyrene particles) and permeation of drug was determined as described previously (Figure 9). Consistent with the findings above, statistically significant increases in permeation rates of fluorescein and rhodamine were observed following exposure of mucus to topically applied nanoparticles. The only combination that did not result in permeation increases due to particle treatment was for rhodamine B in the CF-like mucus model (also consistent with observations above).

## Discussion

To the best of our knowledge these studies are the first to demonstrate that exogenous particles topically applied to mucus can disrupt the mucus barrier. This disruption was significant, often yielding greater than 2-fold increases in permeation of fluorescein (MW = 376) and rhodamine B (MW = 479) through different models of mucus.

**Mucus Barrier Properties.** Reconstituted mucus derived from pig gastric, human cervical, and tracheobronchial mucins have similar mucus structures, and have been found to have physiologically relevant compositions and

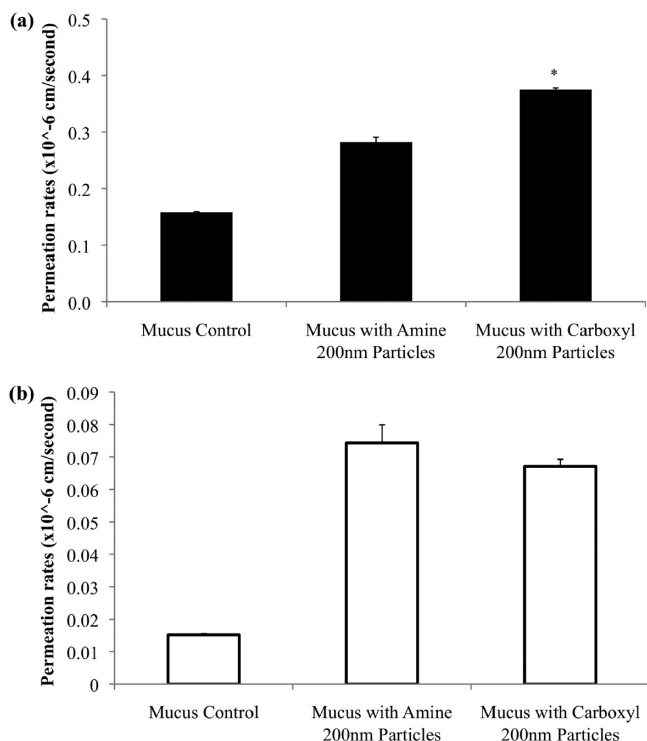


**Figure 5.** Permeation rates of fluorescein (a) and rhodamine B (b) were determined for mucus model that was treated with 200 nm particles with either amine or carboxyl functional groups when compared to control (no treatment). Statistical significance ( $p < 0.05$ ) was seen for fluorescein with carboxylated particles.

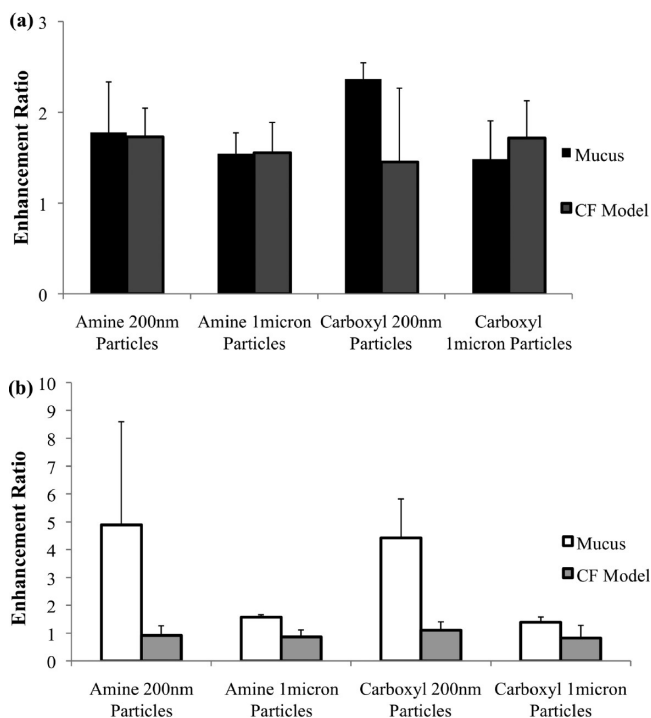


**Figure 6.** Enhancement ratios of either fluorescein (a) or rhodamine B (b) that were used in two different mucus models (mucus versus cystic fibrosis) were compared. rheological properties.<sup>8,9,20</sup> As such several studies have used these models to investigate drug and nanoparticle

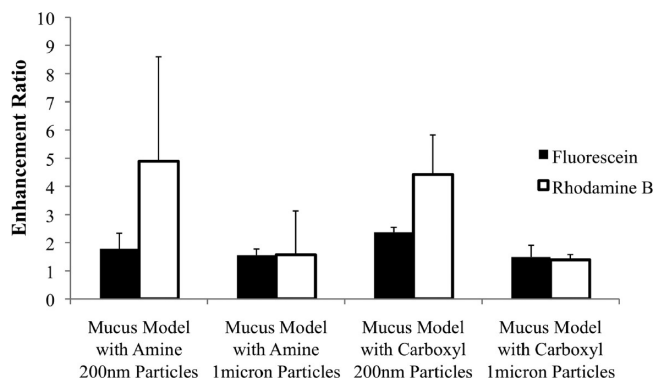


**Figure 7.** Fluorescein enhancement ratios were compared to that of rhodamine B within the mucus model.

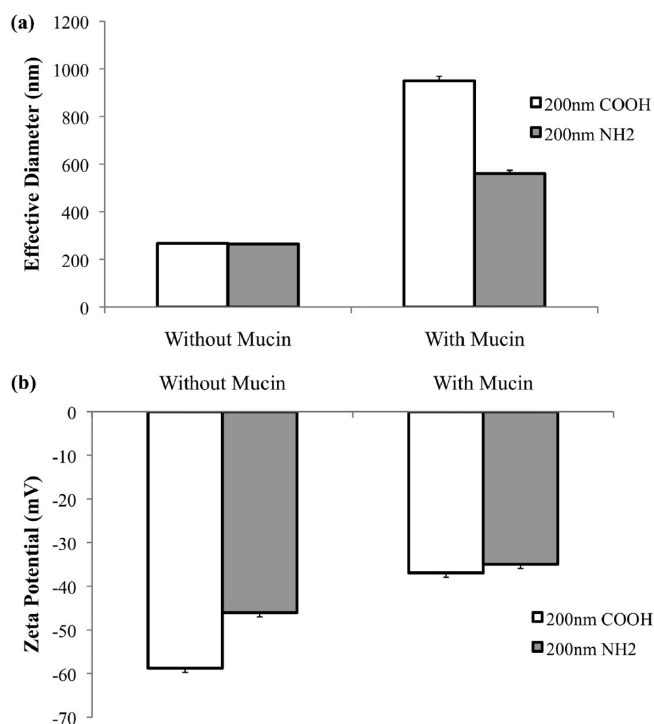


**Figure 8.** Effective diameters were determined by dynamic light scattering (DLS; a) for 200 nm carboxyl and amine functionalized particles before and after mucus treatment ( $n = 3$ ; error bars are standard deviation of the mean). Zeta potentials (b) were then determined using the same conditions as the DLS measurements ( $n = 3$ ; error bars are standard deviation of the mean).

permeability through these barriers.<sup>8,15,19,20</sup> The microstructure of mucus is condensed and represents a highly viscoelastic network that impedes transport of drugs,<sup>8,9</sup> macromolecules,<sup>10,17</sup> nanoparticles,<sup>14,16</sup> gene delivery systems,<sup>12,13</sup> and viruses.<sup>11,17</sup> In some of these studies, the particle interaction with mucus has been explored in more detail.<sup>15–17,20</sup> In these reports, nanoparticles intended as drug and/or gene delivery carriers were entrapped by mucin interactions limiting their transport and inhibiting drug/gene delivery to the target site. These observations are clearly consistent with the intended protective function

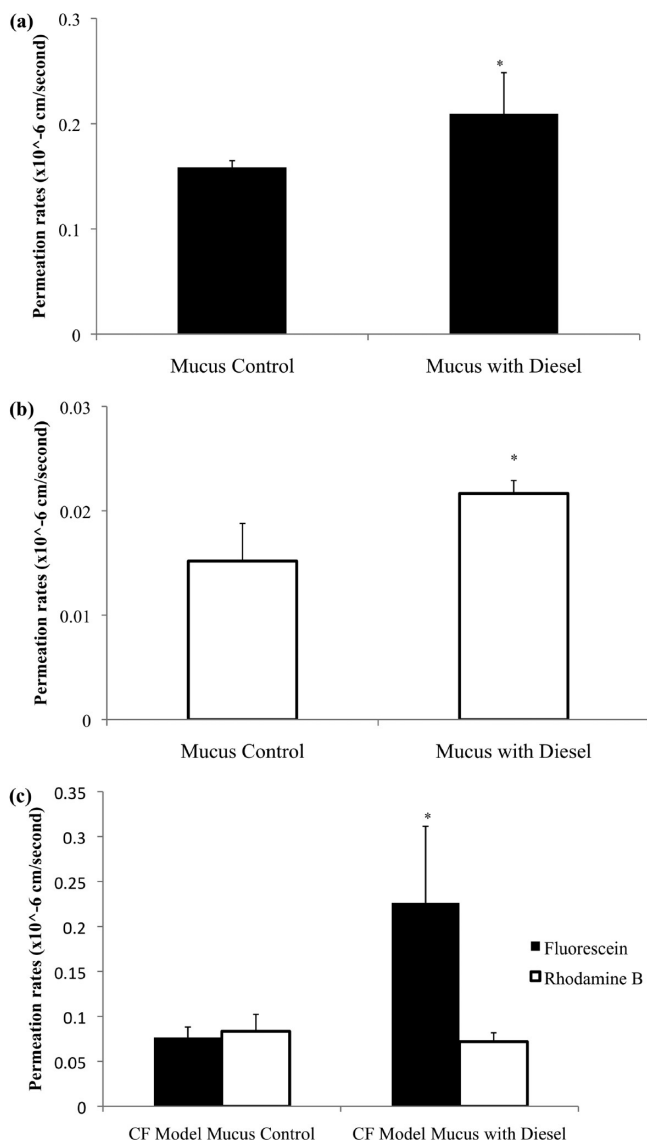


**Figure 9.** Fluorescein (a) and rhodamine B (b) permeability was determined before and after treatment of the mucus model with diesel particulate matter. Statistical significances ( $p < 0.05$ ) were found for both fluorescein and rhodamine B with diesel treatment. Additionally, fluorescein ( $p < 0.05$ ) and rhodamine B permeation rates were determined in the cystic fibrosis mucus model (c).

of mucus, which forms the first and primary barrier on mucosal surfaces.

Using a different approach, we have shown here that particles themselves can interact with mucus and can result in the disruption of the mucus barrier. This particle mediated disruption of mucus leads to modified pathways enabling exogenous substances to pass through the barrier at much faster rates.

**Mucus and Particle Characterization. Mucus Rheology.** Rheological properties of the mucus models were characterized by using the frequency-dependent elastic ( $G'$ ) and viscous ( $G''$ ) moduli. Our studies show that both unpurified and the cystic fibrosis model mucus have increased viscous

modulus at higher frequencies, though the unpurified model had relatively high viscous modulus under all frequencies. Our ranges of  $G'$  and  $G''$  fit within other models of animal mucus, specifically canine respiratory mucus ( $G' = 4.7\text{--}63$  Pa,  $G'' = 1.0\text{--}20$  Pa for subglottis;  $G' = 2.0\text{--}80$  Pa,  $G'' = 0.5\text{--}40$  Pa for tracheal).<sup>22</sup> Canine mucus has been used as a model for human respiratory mucus since the dog lung is similar to the human lung in anatomy and size. Additionally, the tracheal mucus of canine showed similar rigidity to human mucus compared to other animal models (ferret, rabbit, and rat). The mucus models used here were derived from porcine gastric mucins and generally seemed to have consistent ranges of elastic and viscous moduli with those mentioned for pigs ( $G' = 0.18\text{--}160$  Pa and  $G'' = 0.05\text{--}16$  Pa) primarily for the cystic fibrosis model. It should be mentioned that lower shear rates were used since reconstituted mucus tends to deform at lower shear rates than natural mucus.<sup>23</sup> Finally, the bulk  $G'$  determined in our studies is in the same range as those determined in human mucus rheological studies.<sup>18</sup> In summary, the models selected for use in our studies provide viscoelastic properties that match well with literature findings for the physiological mucus.

**Diffusion Barrier Properties.** In addition to rheological characterization of the mucus models, we selected the model drug fluorescein due to its prior use in other studies as a marker of the barrier properties of mucus. Indeed, in the control samples used in these studies, fluorescein exhibited permeability through mucus model barriers similar to other literature results.<sup>8,9</sup> Our experimental setup has small differences in mucus layer thickness, mucus composition, and source compared to other systems described in the literature, and therefore small differences in permeability values were expected.

**Particle Characteristics.** To verify that the particle manufacturer's size and shape specifications were accurate for the different particle systems obtained, scanning electron microscopy (SEM) and dynamic light scattering (DLS) were used. Both methods showed that the particles were close to the size ranges that were described in the product information documentation (200 nm and 1  $\mu\text{m}$ ), though DLS revealed that the particles were slightly larger. The values of the zeta potential of the particles were determined experimentally to be in the range of  $-58.74 \pm 1.66$  mV for carboxyl and  $-46.03 \pm 0.96$  mV for amine particles.

Diesel particulate matter generated from combustion can vary according to the methods used to generate and collect it. Therefore characterization was performed to more clearly define the particle properties. SEM images indicated that the particulate matter were highly aggregated clusters of nanoparticles of various shapes and sizes. When BET surface area was determined, the specific surface area was an average of  $45.0 \pm 0.5$  m<sup>2</sup>/g ( $n = 3$ ). This relatively high specific surface

(22) Lai, S. K.; Wang, Y.-Y.; Wirtz, D.; Hanes, J. Micro- and macrorheology of mucus. *Adv. Drug Delivery Rev.* **2009**, 61 (2), 86–100.

(23) Quraishi, M.; Jones, N.; Mason, J. The rheology of nasal mucus: a review. *Clin. Otolaryngol. Allied Sci.* **1998**, 23 (5), 403–413.



area was expected for these fine particulates given their appearance under the SEM.

**Disruption of Mucus Barrier Induced by Topically Applied Particles.** *Influence of Particle Size.* For the particles chosen for this study two different sizes were used (200 nm and 1  $\mu\text{m}$ ) to assess the potential role of size in mucus disruption. Overall, both particle sizes indicated increased transport compared to controls. However, the effect of nanoparticles on the mucus membrane was greater in magnitude and statistically significant. The nanometer sized particles present a larger surface area for mucin polymer strand contact, and this increased binding area could result in more extensive interactions. These increased interactions may be responsible for the higher permeation rates of drug through the mucus models presented in our data. Our working hypothesis is that the mesh network of mucus is disrupted by the entrapment of particles because the mucin strands collapse onto the particle surface, opening adjacent pores in the mesh. We imagine this interaction to be similar to that seen when an object becomes stuck in a sticky spider's web and, over time, more and more web strands irreversibly bind to the object's surface, causing larger holes to appear in the overall structure of the web.

*Influence of Surface Chemistry.* Particle surface labeling of either amine or carboxyl groups was used to determine any influences these surface groups may have on mucus disruption. Though slight differences in drug permeation were seen between the two surface groups, none were statistically significant, indicating that there was little effect of amine or carboxyl groups on mucus disruption. From our data it can be determined that negatively charged particles, despite the different functional groups used, have the ability to modify the mucus barrier to allow for increased permeation of the model drugs. Dawson et al. and Olmsted et al. previously found that the same polystyrene particles used in our study exhibited significantly hindered transport rates within mucus.<sup>17,20</sup>

*Influence of the Model Drug Properties.* The different model drugs had significantly different permeation rates through the unpurified mucin model, more so than through the CF-like mucin model. The model drugs used were fluorescein sodium salt, a hydrophilic water-soluble fluorescent probe, and rhodamine B, a more lipophilic, water-soluble probe. Rhodamine B transport was the most enhanced when the unpurified mucus barrier was pretreated with 200 nm nanoparticles of either functionality. However, in the more surfactant rich CF-like mucus model (containing lecithin and BSA), rhodamine B permeation was not significantly enhanced by particle pretreatment. On the other hand, fluorescein sodium salt showed an increase in permeation rates compared to controls for both the unpurified and CF-like mucin models. Collectively these observations indicate that (1) drug properties can significantly change permeability rates through mucus, (2) drug properties can have significantly different permeation enhancement following mucus barrier disruption, and (3) this behavior is dependent on the composition of the mucus barrier itself. This points to the

nature of the drug diffusion and partitioning interactions with the molecular structure of the mucin molecules. We speculate that the more lipophilic drug encountered significantly more hindered transport in mucus with higher mucin content due to partitioning into the lipophilic domains of the mucin. CF-like mucus, a model mucus based on compositional analysis of CF sputum samples, contains high amounts of surface active molecules such as lecithin and BSA. Here the permeability enhancement difference for a lipophilic drug was lost, perhaps due to the less defined hydrophilic–lipophilic molecular structure of the barrier in the presence of surfactants. The hydrophilic drug demonstrated significant permeation enhancement following particulate disruption of the mucus regardless of the mucus model. The relatively large error bars seen in the permeation enhancement graphs are likely due to the mucus model composition. Even though these mucus models (CF-like and model mucus) were prepared *in vitro*, they retain some heterogeneity in composition and nonuniformity of the rehydrated mucin polymers. Therefore, the relatively large error bars illustrate expected variabilities in drug diffusion or enhancement within these heterogeneous systems.

**Possible Molecular Mechanisms of Disruption.** In these studies we also investigated possible evidence for direct interactions between the particles and the mucus. Size and charge characteristics of the particles were determined both before and after interaction with mucus using dynamic light scattering (DLS) and zeta potential, similar to the method used by Dawson and colleagues.<sup>20</sup> Particles that had been incubated in mucus (and centrifuged and extensively washed) showed a statistically significant increase in their particle size. Furthermore, following mucus incubation, carboxylate particles and aminated particles appeared to be coated with mucin such that any differences in zeta potentials were eliminated ( $-36.94 \pm 1.57$  mV and  $-39.03 \pm 0.77$  mV respectively). Prior to incubation these particle types had significantly different initial zeta potentials ( $-58.74 \pm 1.66$  mV for carboxyl particles and  $-46.03 \pm 0.96$  mV for amine particles). These results suggest that particles adsorb mucin to their surfaces with strong interactions resistant to centrifugal separation and washing procedures, with limited aggregation. Though DLS data showed some differences with particles incubated with mucus, this may indicate some aggregation has occurred due to either the centrifugation process or mucus interactions with the particles themselves.

Considering these changes in particle properties following exposure to mucus with the patterns of permeation enhancement described above, we speculate that mucus disruption due to topical application of exogenous particles results from direct disturbance of the mesh network of the mucus barrier. Specifically, we imagine the creation of larger holes and diffusional pathways via collapse of mucin strands onto the high surface area of nanoparticles. This scheme is depicted in Figure 1.

The observation of mucin fibers collapsing onto particles was demonstrated by Olmstead and group.<sup>17</sup> They found that



herpes simplex virus (HSV) particles would adhere to cervical mucin fibers causing the fibers to collapse around the HSV particles into dense cable-like structures. Larger porous regions formed around the cable-like structures of the mucin. According to Dawson and co-workers particles that were formulated with cationic PLGA and dimethyldioctadecylammonium bromide (DDAB) were able to be transported faster through mucus compared to COOH-polystyrene particles, despite aggregation of the particles within the mucus.<sup>20</sup> They speculated that the surface chemistries of the two particle types could affect the transport rates. The slightly larger PLGA-DDAB nanoparticles with higher hydrophilicity may predispose them to greater transport within hydrophilic mucus pores. It was also mentioned that the PLGA-DDAB/DNA nanoparticles may result in the collapse of the mucin fiber strands onto the particle surface and thus causing larger pores. This is consistent with our findings where these induced pores would promote increased transport through mucus.

We observed that the surface chemistry of the particles used in this study had little effect on the transport rates of either fluorescein or rhodamine B through mucus. As demonstrated by zeta potential and particle size measurements, it appears that mucin interactions with the particles, despite different surface functionalization, resulted in coating of the particles with mucins that eliminates differences in particle charge (while inducing increases in particle size). Though both particle types were found to be negatively charged, based on zeta potential, it is therefore not surprising that we observed little effect of surface chemistry on drug permeability. Dawson and co-workers also observed the adsorption of mucin fibers to the surfaces of different particle types that resulted in elimination of the differences in surface chemistry.<sup>20</sup> Therefore, mucin appears indiscriminate in its interactions with particles of different surfaces and can entrap exogenous particles regardless of composition differences that would be necessary to protect from the potentially diverse environmental exposures organisms may be subject to. It must also be noted that Hanes and co-workers have described approaches to overcome these interactions using polyethylene glycol of specific molecular weights and coating densities.<sup>16</sup>

The impact of these findings extends beyond drug delivery systems. For example, environmental particulate matter has significant fractions of material in the size and surface area range discussed in this paper. In our initial investigations we selected diesel particulate matter. This nanoparticle system also caused a similar mucus barrier disruption effect indicating that environmental pollutants may also cause mucus modification. This particle induced barrier disruption via inhaled environmental particles has, to the best of our knowledge, not been reported in the scientific literature but has significant implications for allowing increased exposure to other inhaled substances (microbes, carcinogens, etc). Studies investigating these effects are currently underway in our laboratory.

## Conclusions

Based on these data, our working hypothesis is that topically applied particles, such as inhaled pollutants, environmental aerosols, and drug delivery systems, may compromise the mucus barrier via strong association of the biopolymers with the surfaces of the particles leading to the opening of new diffusion pathways through the barrier. With this in mind, the potential effects of this compromised barrier may be important in infectious disease, nanotoxicology, and drug delivery and warrant further investigation.

**Acknowledgment.** The authors would like to acknowledge Stephen Marek for providing the SEM images and Martin Donovan for the illustration for the manuscript. In addition, the assistance of Therapeutex, Drug Dynamics Institute, University of Texas, in obtaining the rheological properties of the mucus models is acknowledged. We also acknowledge Jacob McDonald from the Lovelace Respiratory Research Institute for supplying the diesel particulate matter used.

**Note Added after ASAP Publication.** This manuscript was originally published on the Web on October 15, 2010. The corrected version was reposted with changes throughout on October 20, 2010.

MP100242R